



HAL
open science

Turbulence Patch Identification in Potential Density or Temperature Profiles

Richard Wilson, Hubert Luce, Francis Dalaudier, Jacques Lefrère

► **To cite this version:**

Richard Wilson, Hubert Luce, Francis Dalaudier, Jacques Lefrère. Turbulence Patch Identification in Potential Density or Temperature Profiles. *Journal of Atmospheric and Oceanic Technology*, 2010, 27 (6), pp.977-993. 10.1175/2010JTECHA1357.1 . hal-00458343

HAL Id: hal-00458343

<https://hal.science/hal-00458343>

Submitted on 23 Nov 2020

HAL is a multi-disciplinary open access archive for the deposit and dissemination of scientific research documents, whether they are published or not. The documents may come from teaching and research institutions in France or abroad, or from public or private research centers.

L'archive ouverte pluridisciplinaire **HAL**, est destinée au dépôt et à la diffusion de documents scientifiques de niveau recherche, publiés ou non, émanant des établissements d'enseignement et de recherche français ou étrangers, des laboratoires publics ou privés.

Turbulence Patch Identification in Potential Density or Temperature Profiles

RICHARD WILSON

*UPMC, Université Paris 6, Paris, and Université de Versailles St. Quentin, Versailles,
and CNRS/INSU, LATMOS-IPSL, Paris, France*

HUBERT LUCE

Université du Sud Toulon-Var, and CNRS/INSU, LSEET, La Garde, France

FRANCIS DALAUDIER

Université de Versailles St. Quentin, Versailles, and CNRS/INSU, LATMOS-IPSL, Verrières le Buisson, France

JACQUES LEFRÈRE

*UPMC, Université Paris 6, Paris, Université de Versailles St. Quentin, Versailles,
and CNRS/INSU, LATMOS-IPSL, Paris, France*

(Manuscript received 13 July 2009, in final form 2 November 2009)

ABSTRACT

The Thorpe analysis is a recognized method used to identify and characterize turbulent regions within stably stratified fluids. By comparing an observed profile of potential temperature or potential density to a reference profile obtained by sorting the data, overturns resulting in statically unstable regions, mainly because of turbulent patches and Kelvin–Helmholtz billows, can be identified. However, measurement noise may induce artificial inversions of potential temperature or density, which can be very difficult to distinguish from real (physical) overturns.

A method for selecting real overturns is proposed. The method is based on the data range statistics; the range is defined as the difference between the maximum and the minimum of the values in a sample. A statistical hypothesis test on the range is derived and evaluated through Monte Carlo simulations. Basically, the test relies on a comparison of the range of a data sample with the range of a normally distributed population of the same size as the data sample. The power of the test, that is, the probability of detecting the existing overturns, is found to be an increasing function of both trend-to-noise ratio (tnr) and overturns size. A threshold for the detectable size of the overturns as a function of tnr is derived. For very low tnr data, the test is shown to be unreliable whatever the size of the overturns. In such a case, a procedure aimed to increase the tnr, mainly based on subsampling, is described.

The selection procedure is applied to atmospheric data collected during a balloon flight with low and high vertical resolutions. The fraction of the vertical profile selected as being unstable (turbulent) is 47% (27%) from the high (low) resolution dataset. Furthermore, relatively small tnr measurements are found to give rise to a poor estimation of the vertical extent of the overturns.

1. Introduction

Small-scale mixing is an important issue for a variety of atmospheric and oceanic processes. In situ measurements of velocity and/or temperature microstructures in

the atmosphere and ocean enable direct estimates of turbulence parameters to be obtained, but such measurements remain difficult, expensive, and sparse (e.g., Alisse and Sidi 2000; St. Laurent and Schmitt 1999).

Thorpe (1977) proposed an elegant method to identify and characterize turbulent patches from in situ measurements by comparing an observed and a sorted vertical profile of potential density (or potential temperature). The stable sorted profile corresponds to a rearranged (reference) profile that can be obtained by adiabatic

Corresponding author address: Richard Wilson, Boîte 102, Université Pierre et Marie Curie, 4 Pl. Jussieu, 75252 Paris CEDEX 5, France.
E-mail: richard.wilson@upmc.fr

displacements. Because a vertical profile of potential density (temperature) in a stably stratified fluid is a monotonic function of depth (altitude), overturns display clear signatures in the difference between the measured and sorted profiles. Such overturns trigger convective instabilities, which in turn produce turbulent mixing. The Thorpe method can a priori be applied to standard soundings, either conductivity–temperature–depth (CTD) measurements in the ocean or lakes (e.g., Thorpe 1977; Galbraith and Kelley 1996; Ferron et al. 1998; Alford and Pinkel 2000) or pressure–temperature (PT) measurements in the atmosphere (Luce et al. 2002; Gavrilov et al. 2005; Clayson and Kantha 2008). Recently, it has been proposed to apply the Thorpe analysis to a huge meteorological radiosondes database to infer the space–time variability of atmospheric turbulence (Clayson and Kantha 2008).

The Thorpe signal is defined at each altitude (or depth) as the signal difference (potential density or potential temperature) between the observed and ordered profiles. The difference of altitude (depth) of a data bin in the observed and sorted profiles defines the Thorpe displacement. Thorpe displacements can be viewed as the vertical distances the observed fluid parcels must be adiabatically displaced so that the fluid becomes gravitationally stable everywhere, the available potential energy reaching a minimum. Thorpe displacements are thus related to the available turbulent potential energy (Dillon 1984). The Thorpe length L_T of an overturn is the root-mean-square (rms) of Thorpe displacements for the considered overturn. The Thorpe length is thought to be proportional to the Ozmidov scale $L_0 = (E_k/N^3)^{1/2}$, where E_k is the kinetic energy dissipation rate, and N is the buoyancy frequency (Ozmidov 1965; Dillon 1982). Several methods have been proposed to relate either E_k or L_T to an eddy diffusion coefficient K (Gavrilov et al. 2005).

The Thorpe scale approach has several limitations, however. For example, ship motions or balloon wake can cause severe errors in perturbing the probe movement or the flow itself. Beyond such problems (not discussed here), instrumental noise is a key issue, because noise can produce potential density/temperature inversions in the observed profile, especially in case of weak background stability. In the present context, an inversion is defined as a localized decrease of potential temperature versus height, or of potential density versus depth, whatever its origin. Following the terminology used by Johnson and Garrett (2004), the term *inversion* will refer to both real and artificial structures in a potential density/temperature profile. The term *overturn* will specifically refer to an inversion resulting from atmospheric motions (turbulence or Kelvin–Helmholtz billows). The selection of artificial inversions as overturns

may result in a dramatic overestimation of the turbulent fraction. The space–time inhomogeneity of turbulence can give rise to diffusion coefficient estimations diverging by several orders of magnitude. It is therefore crucial to apply quantitative procedures to discriminate overturns from inversions produced by noise.

A variety of approaches have been proposed for this objective. Thorpe (1977) rejected displacements for which the Thorpe signal does not exceed a predetermined noise level. Ferron et al. (1998) and Gargett and Garner (2008) defined an intermediate density profile in which the density of neighboring points only differs if the difference between them is larger than a predetermined noise threshold. Also, these authors required an overturn to be an isolated region, that is, a region for which fluid parcels are exchanged with others belonging to the *same* region. Galbraith and Kelley (1996) proposed a series of tests for identifying overturns within CTD profiles. First, they considered limits on the minimum size for overturns to be detectable based on the instrumental noise and density gradient. Second, the authors suggested that the run length, defined as the number of adjacent bins of the Thorpe signal with the same sign, can be a useful diagnostic. They based the selection of overturns on an ad hoc value of the ratio between the observed run lengths and that expected from noise. Timmermans et al. (2003) suggested comparing their observed run lengths to the rms run length expected from a random sequence of Bernoulli trials with probability of $1/2$. Gavrilov et al. (2005) selected data segments (arbitrarily of 12.8-m length) as not affected by the noise by applying two combined criteria: 1) the horizontal structure function at 1 m should exceed twice the noise variance, and (2) a potential temperature increase defined as $L_T d\theta_0/dz$ (where θ_0 is the sorted potential temperature) should exceed twice the noise standard deviation. Piera et al. (2002) proposed another approach. After a wavelet denoising of the data, they estimated the potential displacement errors defined as the standard deviation of displacements induced by random instrumental noise. They then considered a data segment as a part of an overturn from the fraction of displacements exceeding the potential errors within that segment.

Alternatively, Alford and Pinkel (2000) qualified selected inversions as overturns when these inversions were present in both temperature and density profiles. Gargett and Garner (2008) proposed a diagnostic parameter allowing for the elimination of inversions resulting from density spikes. Finally, Galbraith and Kelley (1996) as well as Gargett and Garner (2008) introduced tests for rejecting density inversions caused by time-response mismatches in temperature and conductivity sensors. Such validation methods, mostly relevant in an oceanographic

context, were addressed in a recent paper of Gargett and Garner (2008) and will not be further discussed here.

The selection methods based on a threshold depending on the noise level (amplitude of Thorpe signal, run lengths, and noise-induced displacements) are potentially very effective if measurement noise induces random errors in the sorted profile. The key assumption of these methods is that the errors on the Thorpe signal, or on the Thorpe displacements, induced by instrumental noise are independent. This assumption is questionable, however. For instance, Johnson and Garrett (2004) investigated the effects of noise on run lengths. These authors clearly demonstrated that the run-length statistics are related to both the background stratification and the size of the data sample. They concluded that “comparing the distribution of run-lengths or the rms run-length with that expected from a random uncorrelated series is not a reliable way of distinguishing between signal and noise.”

In the present paper, we propose an alternative method to discriminate overturns from inversions induced by random noise. The method is based on the data range statistics within the detected inversions. The range of a sample is defined as the difference between the maximum and the minimum values in that sample. A statistical hypothesis test enabling for the discrimination of turbulent overturns from noise-induced inversions is described.

The paper is structured as follows. In section 2, the effects of noise upon a sorting procedure are investigated. It is shown that the Thorpe signal and displacements due to noise are not independent. A quantitative criterion for the minimum size an overturn must reach to be detected is derived. In section 3, we describe the selection method of overturns and evaluate its performance through Monte Carlo simulations. Section 4 illustrates the use of the method on an atmospheric profile at low and high vertical resolutions. The conclusions are drawn in section 5.

2. Instrumental noise effects on the Thorpe analysis

a. Basic illustration

Measured density (or temperature) profiles are affected by random instrumental noise. Considering for simplicity a monotonic profile of potential density/temperature to which noise is added, artificial inversions can be produced by the noise only. The probability of occurrence for noise-induced permutations depends on the stratification, on the vertical resolution, and on the noise level (see appendix A).

We consider the signal X (potential density or temperature) regularly sampled along the vertical, that is, $X_i = X(z_i)$, where $z_i = z_0 + i \times \delta z$ is the i th sampled level (altitude or depth); z_0 and δz are an initial level and

the vertical sample step, respectively. A key parameter for quantifying the impact of measurement noise in a sorting procedure is the average of the signal difference between consecutive data bins $\bar{\tau}$ scaled by the standard deviation of instrumental noise σ_N :

$$\bar{\zeta} = \frac{\bar{\tau}}{\sigma_N}, \tag{1}$$

where $\bar{\tau} = \overline{X(z_{i+1}) - X(z_i)}$ and the overbar denoting a spatial averaging operator. Hereafter, the averaged consecutive differences $\bar{\tau}$ will be labeled as the trend, and the ratio $\bar{\zeta}$ as the trend-to-noise ratio (tnr). Considering a data sample of size n , the trend estimate reduces to

$$\bar{\tau} = \frac{1}{n-1} \sum_{i=1}^{n-1} (X_{i+1} - X_i) = \frac{X_n - X_1}{n-1}. \tag{2}$$

It is shown in appendix A that the probability of a noise-induced permutation between two bins can be expressed as a simple function of tnr ζ only. A bulk tnr $\bar{\zeta} \approx 1$ corresponds to standard soundings (CDT or PT) within moderately stratified regions (e.g., Galbraith and Kelley 1996), with $\bar{\zeta} \approx 10^{-1}$ corresponding to microstructure measurements for comparable stratification conditions (e.g., Gavrilov et al. 2005).

Artificial inversions can easily be produced in case of weak stability. Figure 1a shows a synthetic signal (dots) made of two sections with distinct linear trends: a region with small tnr [$\zeta = 0.5 \times 10^{-2}$, from bin 50 to bin 150, is enclosed within a region with larger tnr ($\zeta = 10^{-1}$)]. A normally distributed noise $B \sim N(0, 1)$ is added. There is no overturn in this case. Such staircase profiles are commonly observed in real geophysical flows (e.g., Daludier et al. 1994; Woods 1968; Coulman et al. 1995). The dashed curve of Fig. 1a shows the sorted profile. Within the weakly stratified region, the sorted profile is clearly biased because of the sorting of noise. Figures 1b and 1c show the Thorpe signal and the Thorpe displacements, respectively. The Thorpe signal (displacements) is biased toward positive (negative) values in the lower part of the weakly stratified region and toward negative (positive) values in the upper part of this region. Such vertical distributions for the Thorpe signal or Thorpe displacements are very similar to the ones observed in case of a real overturn. The issue is how to discriminate without ambiguity overturns from such noise-induced inversions.

b. Sorting of a noise sample

To illustrate the impact of the sorting of noise, Fig. 2a shows a sample of 100 independent normally distributed variables $B \sim N(0, 1)$ (dots on left panel). The solid line shows the sorted profile. As expected, the lower part of

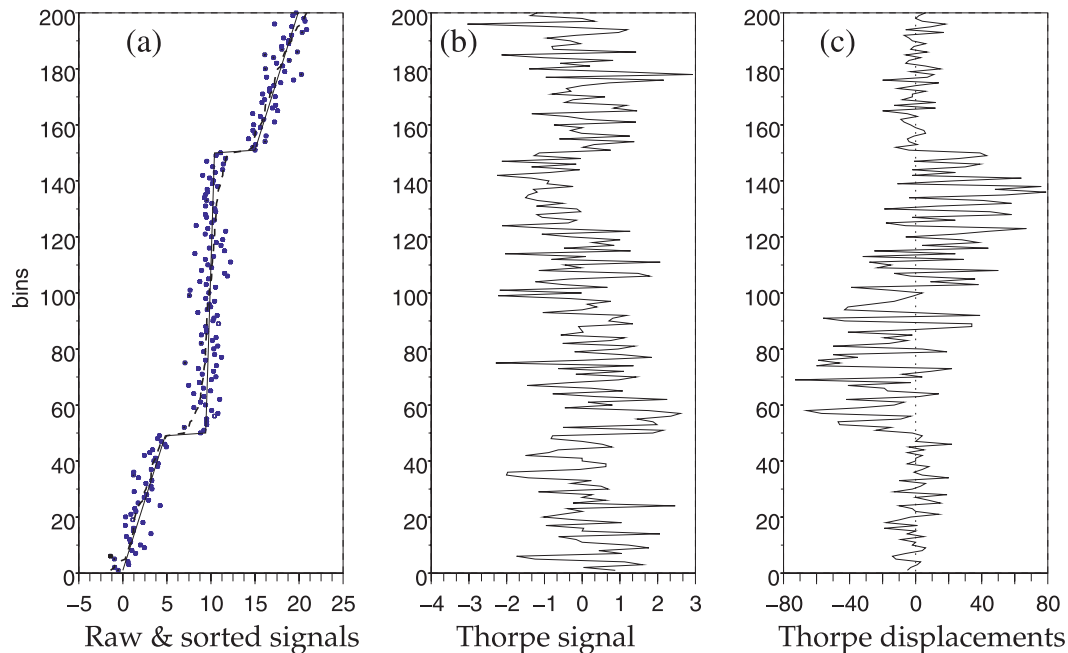


FIG. 1. (a) Raw and sorted synthetic signals. Normally distributed noise is added to a monotonic profile (solid line), the central part of which is weakly stratified. The dashed line shows the sorted profile. (b) The Thorpe signal and (c) Thorpe displacements are shown.

the sorted bins are systematically negative, the upper part positive, and the slope of the sorted profile is positive everywhere. The sorted profile is indeed an empirical estimate of the cumulative distribution function (cdf) of the sample. The dashed curve of Fig. 2a shows the associated theoretical cdf ($\times 100$) for a normally distributed population. The Thorpe signal and the Thorpe displacements are shown in Figs. 2b and 2c, respectively. Clearly, the Thorpe signal or Thorpe displacements of neighboring points are correlated.

The moments of the Thorpe displacements can easily be estimated for such a noise sample. Let $D(i)$ be the difference between the position i and the rank of the i th bin $R(i)$, that is, $D(i) = i - R(i)$. [The Thorpe displacement D_T is simply $D_T(i) = D(i) \times \delta z$.] For n independent, identically distributed (iid) variables, the probability for the i th bin to be at any rank k is simply $1/n$. On the other hand, the possible values for $D(i)$ range between $i - n$ and $i - 1$, that is,

$$\Pr[D(i) = k] = 1/n, \quad -(n-1) \leq k \leq i-1. \quad (3)$$

The displacement $D(i)$ is uniformly distributed: $D(i) \sim U(-n+i; i-1)$, and the mathematical expectation $E[D(i)]$ is

$$E[D(i)] = \frac{1}{n} \sum_{k=-n+i}^{i-1} k = \frac{1}{2}(2i-n-1). \quad (4)$$

For a given bin i , the expectation of displacement for n iid variables depends on position i , but also on the sample size n (dashed curve of Fig. 2c). The sorting of a noisy signal within a neutral (or weakly stratified) region will systematically produce such a positive bias in the reference profile, and thus in the Thorpe signal and Thorpe displacements, making such a region indistinguishable from an overturn (cf. with Fig. 1c).

It is clear from this example that the run-length diagnostic (Galbraith and Kelley 1996) cannot be relevant for such cases. As already noticed by Johnson and Garrett (2004), long run lengths are expected at the top and bottom of weakly stratified regions. The method based on a comparison between Thorpe displacements and noise-induced displacements (Piera et al. 2002) also fails because 1) the displacements due to noise are no longer iid; 2) the noise-induced displacements are not simply proportional to the standard deviation of noise (Fig. 2c); and 3) the mean stratification (from which are estimated the noise-induced displacements), usually evaluated from the sorted profile, is systematically biased (overestimated) due to the sorting of noise (Fig. 2a) if the stability is weak.

c. Size of detectable overturns

As stated by Galbraith and Kelley (1996), a limit in the detection of overturns results from the need to measure density (temperature) differences within overturns

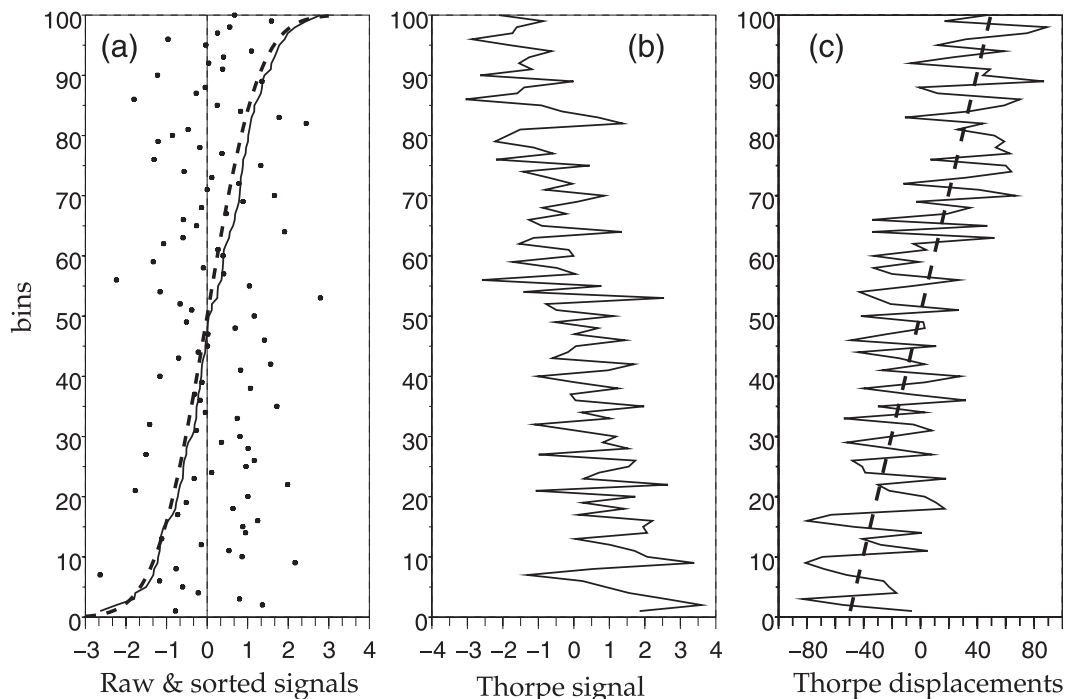


FIG. 2. (a) Raw (dots) and sorted (solid line) noise sample $[N(0, 1)]$. The dashed curve shows the theoretical cdf (\times the sample size) for a normally distributed population. (b) The Thorpe signal and (c) Thorpe displacements are shown, with the dashed line showing the expectation of displacements.

exceeding a threshold imposed by noise and background stratification. However, this threshold not only depends on the noise level but also on the size of the overturn. The difference between the maximum and minimum of the values of a sample defines the sample range W . The statistics of the range for an n sample of iid variables (i.e., random noise) depends on both the probability distribution and the size of the sample n (e.g., David 1981, and appendix B). For instance, Fig. 3 shows the pdf of the range $W_N(n)$ of n iid variables $N(0, 1)$, for $n = 10, 20, 50$ (the subscript N stands for a normally distributed parent population). These pdfs are estimated by numerical integrations of Eq. (B5). As the sample size increases, the pdf of the range is shifted toward larger values and its standard deviation decreases. From these pdfs, various moments and percentiles can be estimated. Figure 4 shows the expectation of the range $E[W_N(n)]$ as well as the 95 and 99 percentiles, w_{95} and w_{99} , respectively, for iid variables, $X \sim N(0, 1)$, as a function of the sample size n for $2 \leq n \leq 5000$ (see also Table 2).

We now consider an inversion of size n , that is, thickness $L_I = (n - 1)\delta z$. To distinguish an overturn from a noise-induced inversion, the range of the data (potential density or temperature) within the inversion $W(n)$ must significantly exceed the range of a noise sample of similar size, $W_N(n)$, that is,

$$W(n) \approx (n - 1)|\tau| \gtrsim \sigma_N W_N(n). \tag{5}$$

The order of magnitude of the minimum τ for an overturn of size n to be detectable is derived from (5):

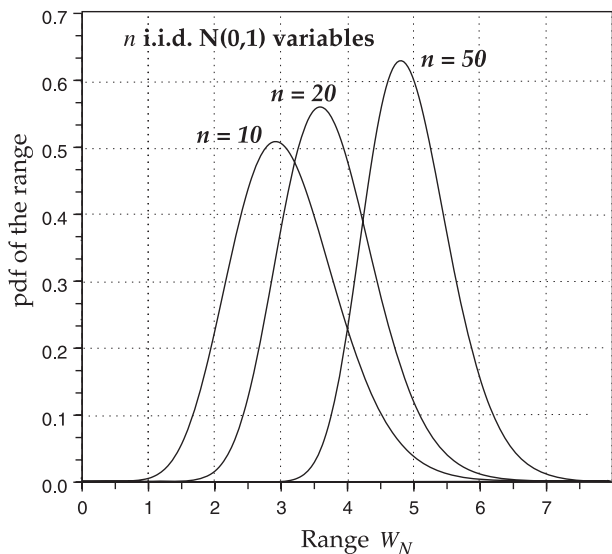


FIG. 3. Theoretical pdf of the range $W_N = \max(X_i) - \min(X_i)$ of n iid variables $X_i, 1 \leq i \leq n$, ($n = 10, 20, 50$). The parent population is normally distributed $N(0, 1)$.

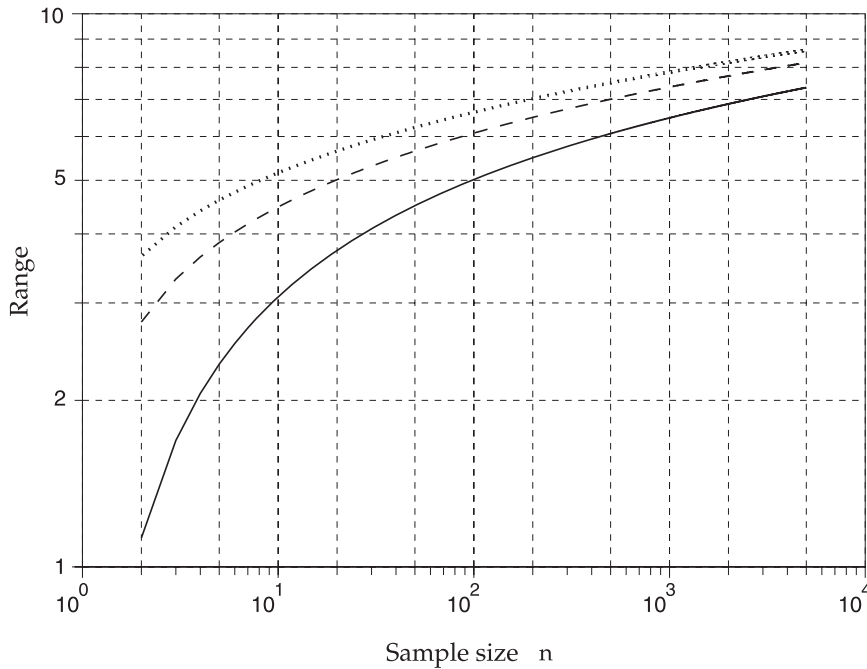


FIG. 4. Expectation of the range $E[W_N(n)]$ of iid $N(0, 1)$ variables vs the sample size n (solid curve). The dashed and dotted curves show the 95th and 99th percentiles, respectively.

$$\left(\frac{|\tau|}{\sigma_N}\right)_{\min} \equiv \bar{\zeta}_{\min} \approx \frac{W_N(n)}{n-1}. \tag{6}$$

Figure 5 shows $\bar{\zeta}_{\min}$ as a function of the sample size n , that is, the size of a detected inversion. The points below the curves are unlikely to be observed, especially if a trend (negative or positive) exists (if any trend exists, the expectation of range is always larger than the expectation for the the null-trend case). For a given tnr , that is, for a given stratification, measurement resolution, and noise level, the curves indicate the minimum length (in bins number) for an overturn to be detectable. For the sake of comparison, the threshold tnr proposed by Galbraith and Kelley (1996) is, with our notations, $\zeta_{\text{GK}} = 2/(n - 1)$ [from their Eq. (5)]. This threshold is shown on Fig. 5 (dotted line). For large inversions, this criterion is too optimistic, as the increase of data range due to the sorting of noise is ignored.

3. Overturn identification

a. The selection procedure

The basic idea of this paper is to infer the existence of an overturn from the range of the signal within the identified inversions (artificial or real). If an inversion is produced by the sorting of noise (H_0 or null hypothesis), the range of the data is expected to be distributed as the range of an n sample of noise. Conversely, if an overturn

is produced within a stably stratified region (H_1 hypothesis), the signal range is expected to exceed significantly the range of a noise sample. Indeed, as the background trend increases, whatever the sign of the trend is, the pdf of the range is shifted toward larger values. A quantitative criterion allowing for the acceptance or rejection of the null hypothesis (H_0) can be obtained by comparing the signal range with the pdf of a noise sample of the same size. The inversion is likely to be an overturn if the signal range exceeds a threshold corresponding to a large percentile of the noise sample. Otherwise, one can not draw a conclusion.

To illustrate our purpose, we build a synthetic signal $X_i, 1 \leq i \leq 100$. Normally distributed noise $B \sim N(0, 1)$ is added to a test model profile. A realization for which $\bar{\zeta} = 0.25$ (and thus $\bar{\zeta} = 0.5$ because $\sigma_N = 1$) is shown in Fig. 6. “Solid-body” and “sine” overturns are simulated from bin 11 to 30 and 71 to 90, respectively (Fig. 6a). A weakly stratified region, from bin 41 to 60, produces an artificial inversion that is clearly visible in the Thorpe displacements profile (Fig. 6d).

To determine the size of the detectable overturns, we first evaluate a bulk tnr . From the trend estimate $\bar{\tau} = X_{i+1} - X_i \equiv (X_{100} - X_1)/(100 - 1)$ and standard deviation of noise σ_N , we deduce $\bar{\zeta} = \bar{\tau}/\sigma_N$ (dashed line of Fig. 6b). A local value for the tnr is estimated from the sorted profile: $\zeta_i = (X_{i+1:100} - X_{i-1:100})/2\sigma_N$, where $X_{i:100}$ is the bin of rank i within the sorted 100 samples (dashed

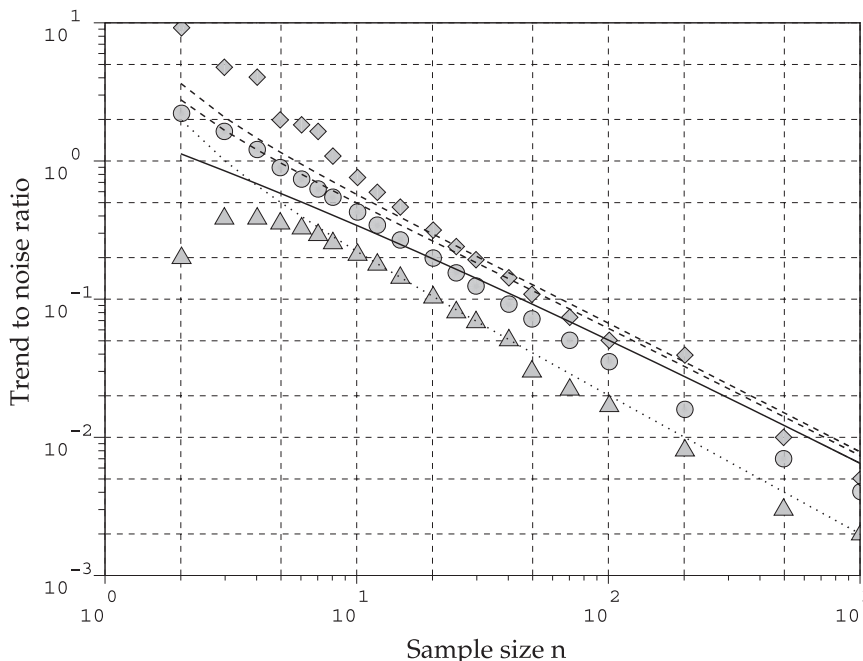


FIG. 5. Relationship between overturn size, n , and threshold $\text{tnr} \bar{\sigma}_{\min}$ for normally distributed noise. The solid curve shows the threshold tnr deduced from the expectation of range W_N . The dashed curves show the thresholds corresponding to the 95th and 99th percentiles. The dotted curve shows the threshold proposed by Galbraith and Kelley (1996). The positions of triangles, circles, and diamonds correspond to test power of 0.1, 0.5, and 0.95, respectively.

curve of Fig. 6a). A minimum of tnr is clearly visible in the central part of the profile, where the stratification is weak. Given the bulk tnr , an order of magnitude for the size of a detectable overturn can be estimated from Fig. 5. From our simulated dataset, the bulk tnr is 0.5 and the size for a detectable overturn is on the order ~ 10 bins (Fig. 5). Consequently, noise reduction is not required because we consider 20 bin inversions in the present case. The noise reduction of data will be discussed in section 4c.

The next step consists of identifying inversions (real and artificial) from the signal (potential density or potential temperature). According to Dillon (1984), an inversion is defined as an isolated region, that is, a region for which $\sum_{k=1}^n D_T(k) = 0$, where n is the size of the inversion. We also required, for any $1 \leq k \leq n$, that $\sum_{i=1}^k D_T(i) < 0$. This last condition implies that the displacements are negative at the bottom of the inversion and positive at the top, as expected for an inversion (taking into account our definition of Thorpe displacements). Owing to this process, both artificial inversions and overturns are selected. Figure 6c shows the cumulative sum of displacements versus bins. Three large inversions are identified at bins 11–30, 41–60, and 71–90. Smaller size inversions are also visible.

The final step consists of selecting the overturns among the detected inversions. The selection method is based

on a statistical hypothesis test. A given inversion is either an overturn (H_1 hypothesis) or not (H_0 hypothesis). If not, the inversion is believed to be induced by noise. The signal range within the detected inversions has to be compared with the range of a noise sample of the same size because the pdf of the range depends on the size of the sample (see Fig. 3). Let $w_p(n)$ be the p percentiles of the range of n iid normally distributed variables, that is, $\Pr[W_N(n) < w_p(n)] = p/100$. By retaining a $p\%$ confidence level, an inversion of size n is recognized as a noise-induced one (H_0 hypothesis) if its data range $W(n)$ is such that

$$\frac{W(n)}{\sigma_N} < w_p(n) \tag{7}$$

and is rejected otherwise (H_1 hypothesis). The probability of rejecting H_0 if H_0 is realized (type I error, corresponding to an erroneous detection) defines the significance level α ($\alpha = 1 - p/100 = 0.05$ or 0.01). The probability β of accepting the H_0 hypothesis when H_1 is realized (type II error, corresponding to the nondetection of a real overturn) depends on the characteristics of the overturns and may be estimated through Monte Carlo simulations (see Table 1). The power of a hypothesis test is usually defined as the probability of rejecting

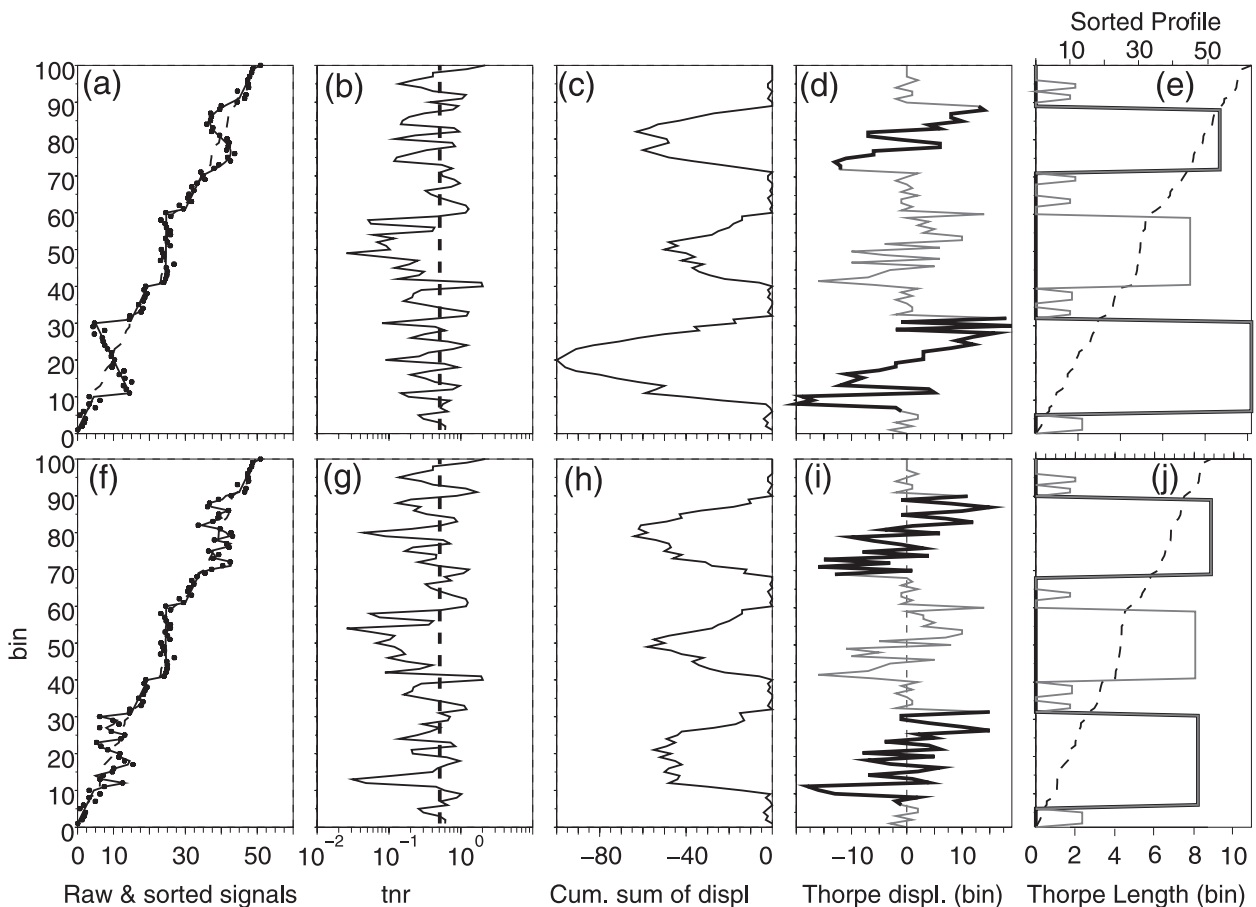


FIG. 6. One realization of a synthetic profile made for a linear trend and additive noise. (top) Solid-body and sine inversions (bins 11–30 and 71–90, respectively) with the central region (bins 41–60) being weakly stratified are shown. (bottom) As in the top, but with fully stirred inversions. (a),(f) The profiles for the solid curve, the dots, and the dashed curve show the signal, the signal plus noise, and the sorted profile, respectively. (b),(g) The tnr for local (solid curve) and bulk (dashed line) estimates. (c),(h) The cumulative sum of Thorpe displacements. (d),(i) Thorpe displacements, with the selected overturns highlighted. (e),(j) Thorpe lengths for the detected inversions, with the sorted profile being superimposed (dashed curve).

H_0 when it is false, that is, to detect an existing overturn, which is equal to $1 - \beta$ (Freeman 1963). The thresholds of range $w_p(n)$ corresponding to significance levels $\alpha = 0.05$ and $\alpha = 0.01$, that is, w_{95} and w_{99} , are plotted in Fig. 4 and tabulated in Table 2. The expectation, standard deviation, as well as various percentiles of the range of a normally distributed population $N(0, 1)$ can be downloaded as an American Standard Code for Information Interchange (ASCII) file (available online at <ftp://ftp.aero.jussieu.fr/pub/os/WN.txt>). If the noise is assumed to follow a distribution other than normal, the percentiles of the range have to be numerically calculated from Eq. (B5).

b. Validation of the hypothesis test

Monte Carlo simulations (1000 runs) were performed from the synthetics presented in the previous section with various bulk tnr values. For the particular realization shown in Fig. 6, for which $\text{tnr} = 0.5$, the detected

inversions extend over about 85% of the profile due to the generation of small size noise-induced inversions.

The thresholds of range corresponding to significance levels of 5% and 1% for a 20-bin noise sample are $w_{95}(20) = 5.01$ and $w_{99}(20) = 5.65$, respectively (Table 2). For a $\text{tnr} \bar{\zeta} = 0.5$, and with a significance level of 1%, the solid-body overturn (bins 10–30) is always detected, (power = 1), the corresponding observed range (mean \pm standard deviation) is $W = 11.9 \pm 1.8$ (here $\sigma_N = 1$). The sine overturn (bins 71–90) for which $W = 7.0 \pm 1$ is identified for 98.1% of the runs (type II error for about 1.9% of the cases). For the artificial inversion (bins 40–60), $W = 3.6 \pm 0.95$. The inversion is selected as an overturn for about 0.7% of the runs (see Table 1). Figure 6 (top panel) shows the position and vertical extent of the overturns as well as the corresponding Thorpe lengths for this particular realization, a case where the two overturns are correctly identified (more than 98% of the cases).

TABLE 1. Results of the Monte Carlo simulations. Here, L_T and inversion widths are expressed in bin units. L1, L2, L3 designate the solid-body, noise-induced, and sine inversions, respectively. The percentage of selected overturns (PSO) shows the power of the test for L1 and L3 overturns.

No stirring				Stirring		
$\bar{\zeta} = 1$						
PSO (%)	L_T	Width	Layer	PSO (%)	L_T	Width
100	11.6	20.9	L1	100	8.2	20.8
0.6	8.1	20.0	L2	0.9	8.8	20.0
100	9.9	20.4	L3	100	9.2	21.9
$\bar{\zeta} = 0.5$						
PSO (%)	L_T	Width	Layer	PSO (%)	L_T	Width
100	11.0	24.3	L1	100	7.8	24.0
0.7	7.8	20.8	L2	0.7	8.2	20.5
98.1	9.7	21.3	L3	99.5	9.0	22.7
$\bar{\zeta} = 0.25$						
PSO (%)	L_T	Width	Layer	PSO (%)	L_T	Width
77.0	9.8	33.8	L1	75.2	7.4	33.9
13.2	7.4	41.5	L2	12.7	7.4	40.2
62.7	8.4	31.7	L3	67.5	8.1	32.5

For $\bar{\zeta} = 1$, 100% of the overturns (solid body and sine) are selected (power = 1) with a 99% confidence level, and 0.6% of the artificial inversions are selected as overturns (Table 1); for $\bar{\zeta} = 0.25$, the power falls down to 0.77 (solid body) and 0.62 (sine). On the other hand, the artificial inversion is selected as an overturn for 13.7% of the cases. Such a large percentage of type I errors are due to the poor detection of the boundaries of the inversions (see the widening of the detected inversions in Table 1). The range test is then applied to samples mixing inversions and “stratified” zones. The test fails.

c. Influence of stirring by turbulence

Within the ocean or atmosphere, overturning layers frequently contain random (turbulent) fluctuations and solid-body or sine overturns are only seldom observed. Furthermore, the cumulative sum criterion applied for the detection of inversions may appear questionable in case of a random distribution of fluid particles positions within the inversions. Another simulation was thus performed by assuming particles randomly distributed within the inversions. Such a complete randomization of the bins’ positions simulates an extreme influence of stirring. Compared to the previous case, the data range remains unchanged within the inversions, but the Thorpe displacements are now fully random (and not only randomized by the noise). It is likely that most of the oceanic or atmospheric overturns lie in between these two extreme cases, from “solid” to “fully stirred” overturns.

TABLE 2. Moments and percentiles of the range for n iid with normal $N(0, 1)$ pdf.

n	$E[W_N]$	$\sigma[W_N]$	w_{95}	w_{99}
2	1.13	0.85	2.77	3.64
3	1.69	0.89	3.31	4.12
5	2.33	0.86	3.86	4.60
7	2.70	0.83	4.17	4.88
10	3.08	0.80	4.47	5.16
12	3.26	0.78	4.62	5.29
15	3.47	0.76	4.80	5.45
17	3.59	0.74	4.89	5.54
20	3.73	0.73	5.01	5.65
25	3.93	0.71	5.17	5.79
30	4.09	0.69	5.30	5.91
35	4.21	0.68	5.41	6.01
40	4.32	0.67	5.50	6.09
45	4.42	0.66	5.58	6.16
50	4.50	0.65	5.65	6.23
60	4.64	0.64	5.76	6.34
70	4.75	0.63	5.86	6.43
80	4.85	0.62	5.95	6.51
100	5.02	0.60	6.09	6.64
120	5.14	0.59	6.20	6.74
150	5.30	0.58	6.33	6.86
200	5.49	0.57	6.50	7.02

As mentioned previously, we performed 1000 runs with various bulk tnr but with stirred inversions. The lower panels of Fig. 6 show the results of the selection procedure for the same particular realization (upper panels) but with fully stirred inversions. No significant difference was noticed, neither in the inversions detection nor the fraction of selected overturns (Table 1). The Thorpe length estimate does not seem to be affected much by the assumed complete stirring, although it is slightly smaller in case of a solid-body overturn. Also, the shape and amplitude of the cumulative sums of displacements are now roughly the same for the three main inversions (Fig. 6h). Therefore, one can conclude that the proposed selection criterion for the detection of overturns does not depend on the presence (or importance) of stirring within the inversions.

Results of Monte Carlo simulations for three different bulk tnr $\bar{\zeta}$ and $n = 20$ are summarized in Table 1. Clearly, for $n = 20$ the selection method is not effective if $\bar{\zeta} < 0.5$ because inversions are not correctly resolved (one observes an increase in width of the detected inversions). For the extreme case $\bar{\zeta} = 0$ (shown in Fig. 2) the whole profile is recognized as a single inversion.

d. Power of the hypothesis test

For a fixed inversion size ($n = 20$), the power of the test is observed to increase with tnr $\bar{\zeta}$. It also likely depends on n . The power of the test was estimated through Monte Carlo simulations for $2 \leq n \leq 1000$, and $0.001 \leq \bar{\zeta} \leq 1.0$.

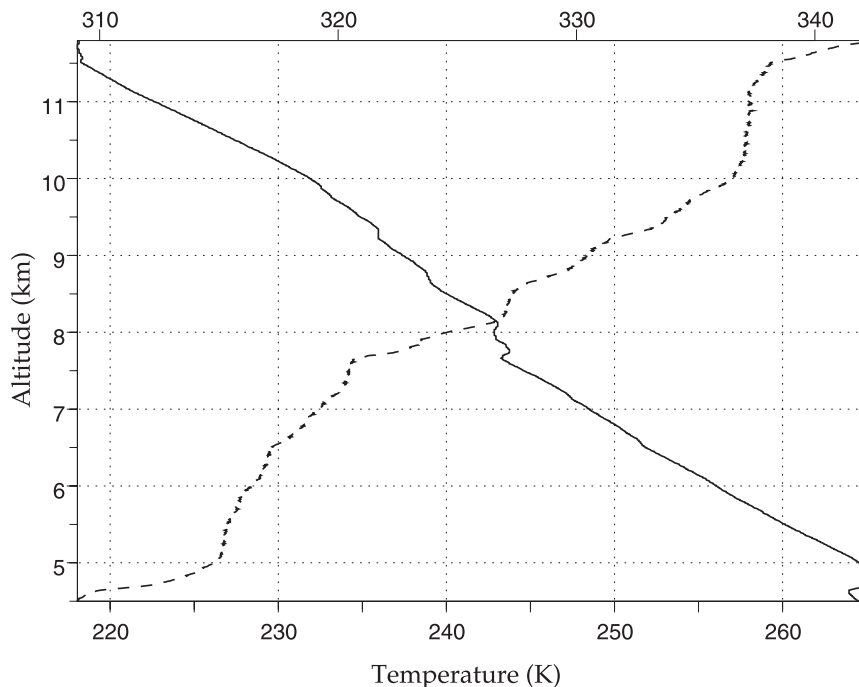


FIG. 7. Temperature in the upper troposphere (solid line and bottom scale) measured by the RS90G Vaisala radiosonde launched on 13 May 2000 at Kyotanabe, Japan, during the MUTSI campaign. The dashed line (top scale) shows the corresponding potential temperature.

The size–tnr coordinates for which the test power is 0.1, 0.5, and 0.95 are shown as symbols in Fig. 5. Clearly, the power is an increasing function of both n and $\bar{\zeta}$. For a considered size n , the power is increasing from 0 to 1 starting from a tnr threshold depending on n . Identically, the power is increasing with n for constant $\bar{\zeta}$. For large overturns ($n > 50$), the test power is high (>0.9) for the tnr values corresponding to a significance level 0.05 or 0.01 (dashed curves). Conversely, for the small overturns ($n \leq 10$) the power is only slightly larger than 0.5 for the threshold tnr.

4. Example with real atmospheric data

a. Dataset description

The proposed selection procedure is now applied to vertical profiles of atmospheric temperature and pressure. We used data collected from a RS90G Vaisala radiosonde launched during a radar-balloon observation campaign called the Middle and Upper Atmosphere (MU) Radar, Temperature Sheets, and Interferometry (MUTSI; Luce et al. 2002; Gavrilov et al. 2005). The initial sampling frequency and vertical resolution (after resampling at a constant vertical step) were 0.69 Hz and 6 m, respectively. High-resolution (HR) balloon measurements were also performed with sampling frequency and vertical resolution of 50 Hz, and ~ 10 cm, respectively.

The reader can find more details about the HR measurements in Gavrilov et al. (2005). By contrast, the Vaisala data will hereafter be labeled as low-resolution (LR) data. The HR and LR sensors were on the same gondola, and the data were collected simultaneously.

Figure 7 shows a vertical profile of tropospheric temperature measured on 13 May 2000. The potential temperature θ is inferred from the measured temperature and pressure using the relation for ideal diatomic gas:

$$\theta = T \left(\frac{1000}{P} \right)^{2/7}, \quad (8)$$

where T is the temperature (K) and P is the pressure (hPa). Several nearly neutral layers can be seen around 4-km altitude and above 10-km altitude.

In the present work, we consider tropospheric data only (from 4.5- to 11.8-km altitude), that is, data acquired in relatively weak stability (low tnr) conditions. The noise is evaluated experimentally from the temperature measurements for both LR and HR data: after the removal of a linear trend on short data sequences (five points), we calculated the mean of the squared data differences. The average from all the sequences is an estimate of twice the noise variance. The standard deviation of noise for LR (HR) temperature measurements is found to be 22 (2.2) mK. The noise level of the observed

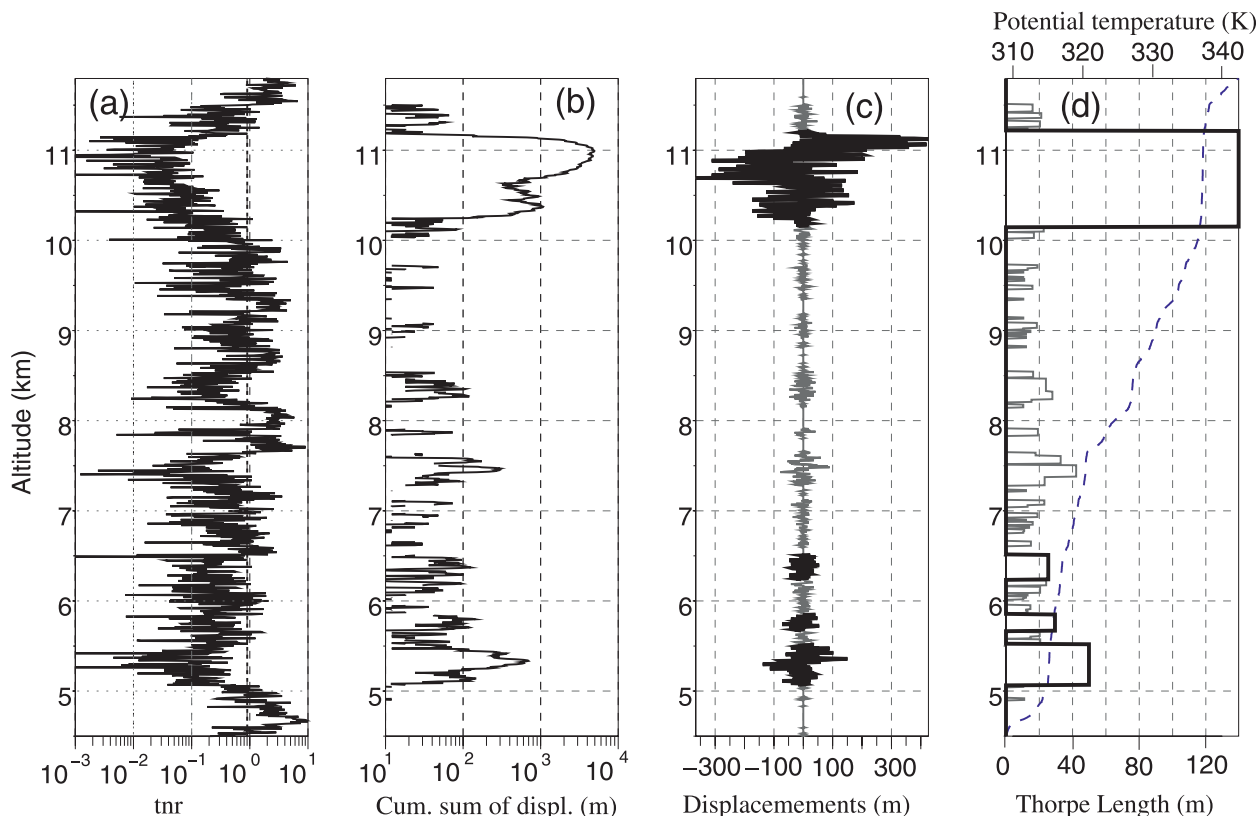


FIG. 8. LR data: (a) tnr, the dashed line showing the bulk tnr; (b) absolute value of the cumulative sum of displacements; (c) Thorpe displacements, with the selected overturns highlighted; and (d) Thorpe lengths for the detected inversions (gray), with selected overturns highlighted. The sorted potential temperature profile is superimposed (dashed).

temperature data is independent of altitude, whereas the noise level of the potential temperature slightly varies with altitude because of the pressure term [Eq. (8)]: it increases from 26 to 35 (2.6–3.5) mK for LR (HR) data for heights ranging from 4.5 to 11.8 km.

The vertical profile of tnr for the LR data is shown in Fig. 8a. The bulk tnr $\bar{\zeta}_{LR}$ is ~ 0.9 (dashed line), the local values showing minima less than 10^{-1} around 11-km altitude. For such a bulk tnr, one cannot expect to detect overturns smaller than $n \sim 6$ bins, that is, thinner than 30 m (Fig. 5). Furthermore, the test power reaches 0.95 for $n \sim 10$ (54 m). Within the low stability region, the threshold size is ~ 70 bins (414 m). The bulk tnr of the HR measurements is $\bar{\zeta}_{HR} \sim 0.14$, so detectable size is $n \sim 50$ bins (5 m), with test power reaching 0.95 for such a size. As shown later in the study, a denoising procedure can provide better performances.

b. LR data analysis

Figure 8 shows the Thorpe displacements (Fig. 8c) and the cumulative sum of displacements (Fig. 8b) for the LR data. The Thorpe displacements range from

about 10 to 300–400 m. For this particular profile, the (real and artificial) inversions extend over 60% of the upper troposphere.

By applying the selection test with a 1% significance level, about 91% of the inversions are not selected as overturns. The turbulent fraction, that is, the fraction of the profile which is selected as overturns, falls down to 27%. The four selected turbulent patches are shown in Fig. 8d (thick lines); here the Thorpe lengths for the detected inversions with the selected (presumably turbulent) overturns are highlighted. The sorted potential temperature profile is superimposed on the figure. A thick turbulent region is observed from altitudes 10.1–11.2 km, with a Thorpe length of about 140 m. Thinner layers are also observed below 6.5 km, with Thorpe lengths ranging from 25 to 50 m. It is worth noting that most of the inversions are not selected as overturns: for their given tnr and sizes, their ranges cannot be distinguished from the range of random noise samples. Of course, a less restrictive confidence level can be used, at the expense of a larger rate of (accepted) errors. For $\alpha = 25\%$, the ratio of selected overturn is 21%, and for $\alpha = 25\%$, it reaches 40%.

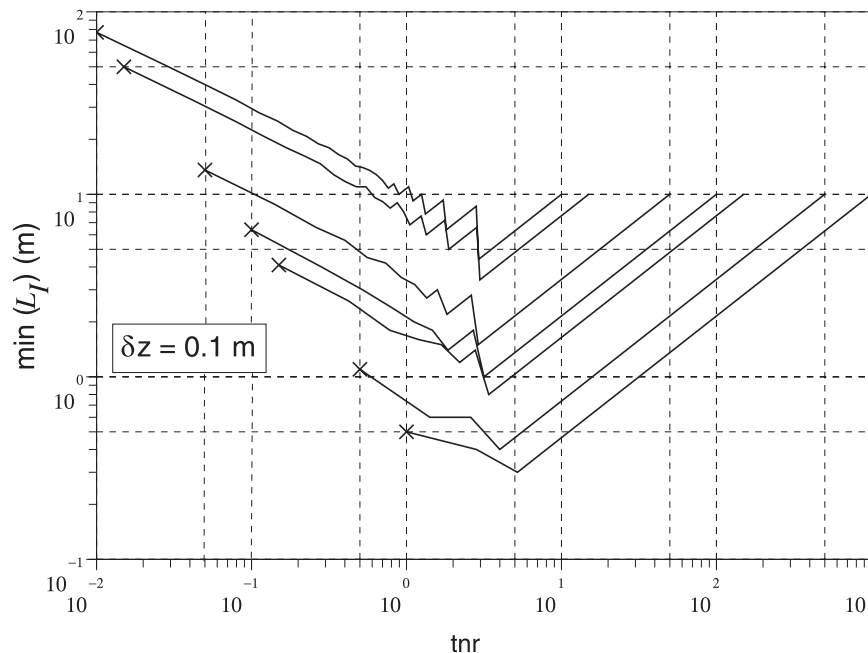


FIG. 9. Minimum size of detectable overturn L_I (m) vs tnr of filtered and undersampled data for various initial (raw data) tnr values (indicated by crosses). Here, L_I depends upon the initial vertical resolution δz [$L_I = (n - 1)\delta z$].

c. Denoised HR data analysis

As mentioned previously, $\bar{\zeta}_{\text{HR}} \sim 0.14$, the detectable size for an overturn with 1% significance level being $n \approx 50$ bins (5 m). Also, for such a low tnr the vertical extent of turbulent overturns is likely poorly resolved. A denoising procedure aimed to increase $\bar{\zeta}$ is required. One difficulty lies in the need to preserve the independence of the data bins to compare the signal range with the range of an iid noise sample (we do not know how to estimate the range of correlated noise). A crude and sufficient method would consist of reducing the data resolution; to subsample by a factor m , increases $\bar{\zeta}$ by the same factor. Because the data bins remain independent after undersampling, the range test can still be applied on undersampled data. Second, smoothing out the data with a running window of length m reduces the standard deviation of noise by a factor $\sim m^{-1/2}$, thus increasing $\bar{\zeta}$ by a factor $m^{1/2}$. Consequently, a simple way to increase the tnr by a factor $m^{3/2}$, while keeping the noise uncorrelated, consists of 1) smoothing out the profile with a running filter of size m and 2) undersampling the smoothed profile by the same factor m .

The size of the running window (undersampling factor) must be chosen to optimize the procedure. It is expected that, above a certain tnr value, the minimum detectable size of overturn reaches 2 bins. A further downsampling is useless because a degradation of the vertical resolution

will only lead to an increase of the smallest size of the detectable overturn. Figure 9 shows the size of the detectable overturn (m) versus the tnr ζ of the subsampled data for various initial (raw data) tnr values. An optimum is found for $3 \leq \zeta \leq 5$.

Based on this empirical result, the HR potential temperature profile has been smoothed out with a 9-point Hamming window and resampled at a vertical step of nine bins (0.9 m). This procedure increased $\bar{\zeta}_{\text{HR}}$ by a factor $\sim 9^{3/2} = 27$, that is, $\bar{\zeta}_{\text{HR}} \approx 4$ (Fig. 10a).

The selected turbulent overturns from the degraded HR data are shown in Fig. 10d. The contrast with the results obtained from the LR data (Fig. 8) is striking: the turbulent fraction is now 47% (27% from the LR data). A large fraction of small size overturns are selected from the HR data and Thorpe lengths are also much smaller, ranging from ~ 5 to 140 m. Although not surprising in regions where inversions are not detected from the LR profile (because the resolution of the degraded HR data is about 6 times better), overturn sizes and Thorpe lengths are also observed to be smaller in the 5–6.5-km altitude domain, where overturns are detected from both datasets. One also observes that the thick turbulent patch selected from LR data (from 10.1 to 11.2 km) is now split into several patches, the thicker one having about 300-m depth. However, the Thorpe lengths for this large overturn are similar from both datasets.

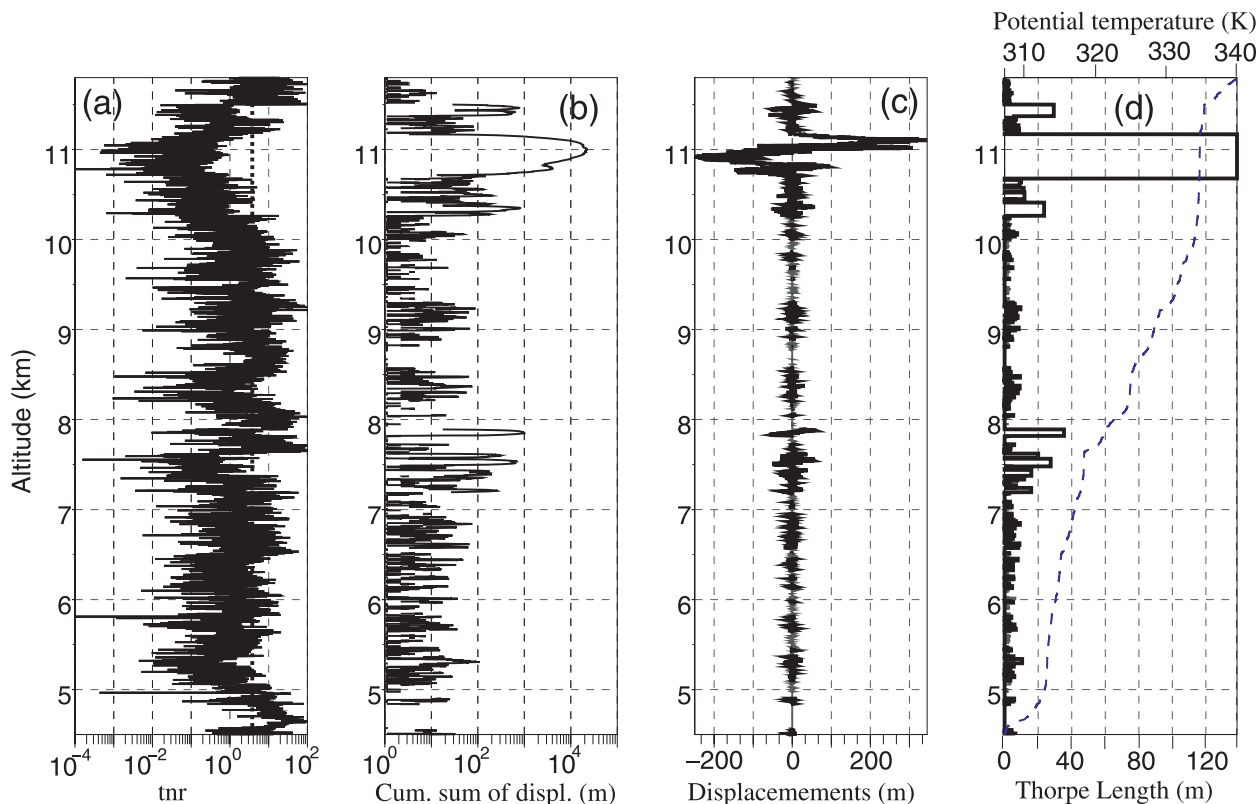


FIG. 10. As in Fig. 8, but for the undersampled and filtered HR data.

The large differences in the size of the selected overturns are very likely a consequence of the poor precision in the evaluation of their vertical extent for low tnr data. The tnr of LR data is so small within the 10–11-km altitude domain, $\zeta_{LR} \sim 10^{-1}$, that a widening effect due to the large probability of noise-induced permutations is likely to occur (see appendix A and Fig. A2). For instance, with $\zeta = 0.1$ the probability for a permutation due to noise between adjacent bins is 0.46 and remains as large as 0.3 for two bins five steps apart (Fig. A2).

5. Summary and conclusions

The present work was motivated by the need for a robust procedure applicable to Thorpe analyses aimed to distinguish real overturns from inversions produced by instrumental noise. For this purpose, we build a hypothesis test based on the statistics of the data range. The theory of order statistics was presented by David (1981), and the fundamentals of the range statistics are recalled in appendix B.

The procedure for selecting overturns consists of three steps:

- 1) We first estimate the bulk tnr [Eqs. (1) and (2)], which gives an indication on the minimum size (in bin

- numbers) for the detectable overturns [Eq. (6) and Fig. 5]. If this size is too large, a preliminary denoising procedure is required (section 4c).
- 2) The Thorpe displacement profile is constructed. The noise-induced and real inversions are detected within the profile from the cumulative sum of the Thorpe displacements.
- 3) An inversion is selected as an overturn if its range exceeds a large prescribed percentile of a noise sample of the same size [(Eq. (7)). For practical purposes, we tabulated the moments, as well as various percentiles, of the range for normally distributed variables as a function of the sample size [Table 2 and an ASCII file (available online at ftp://ftp.aero.jussieu.fr/pub/os/WN.txt)].

The statistical test was validated through Monte Carlo simulations for various tnr values and inversion sizes and by assuming stirred and nonstirred inversions. The probability for an erroneous selection (type I error) is limited by a prescribed significance level α , usually 0.05 or 0.01. The power of the test, that is, the percentage of correctly detected overturns, is found to be an increasing function of both the tnr and the size of the inversions (Fig. 5).

The denoising procedure is based on the degradation of the vertical resolution of the original data. It aims at

increasing the tnr although preserving the independence of the noise between data bins. The tnr of the degraded data increases by a factor $m^{3/2}$, where m is the under-sampling factor (i.e., the number of bins of the running filter). The parameter m is constrained by a trade-off between the desired detectable size of overturns and the reliability of the selection test (quantified through its power).

To illustrate our purpose, the selection procedure was applied to two datasets obtained simultaneously during a single balloon flight: 1) a low-resolution (LR) profile with vertical resolution $\delta z = 6$ m and a bulk tnr $\bar{\zeta}_{\text{LR}} \sim 0.9$, and 2) a high-resolution (HR) profile with $\delta z = 0.1$ m and $\bar{\zeta}_{\text{HR}} \sim 0.14$. From the LR dataset, the size of detectable overturns with a significance level $\alpha = 0.01$ is $n \sim 6$ bins, that is, 30 m (Fig. 5). For such a size, the probability of overturn detection, that is, the power of the test, is about 0.5. A power of 0.95 can be obtained by increasing the detectable size up to 10 bins (54 m). For the HR profile, with the same significant level and 0.95 power, the detectable overturns size is $n \sim 50$ (5 m).

Clearly, overturns of a smaller size can be detected from the HR profile if a denoising procedure is applied. By degrading the vertical resolution to 0.9 m ($m = 9$), the bulk tnr is increased to $\bar{\zeta} \sim 4$, which is an optimal value (Fig. 9). For such a tnr, one can theoretically detect two bins' overturns (0.9 m) with a high confidence (Fig. 5).

Major differences in the distribution of sizes of the selected overturns are observed from these two datasets (Figs. 8 and 10). Not surprisingly, smaller overturns are selected from the HR profile, the selected turbulent fraction are almost twice as large (45% versus 27%), with most of the HR selected overturns being thinner than 100 m. The results demonstrate the importance of HR measurements with high tnr for determining the turbulent fraction of the atmosphere. The difference in the size of the overturns selected within the same altitude domain from both datasets is likely a consequence of the poor determination of the boundaries of the overturns (defined as isolated layers) for low tnr conditions ($\bar{\zeta}_{\text{LR}} \ll 1$ where overturns are detected). This effect is also visible from the Monte Carlo simulations; see, for instance, the relative widening of the detected overturns for low tnr conditions (Table 1). Consequently, the size distribution of the selected overturns appears to be very sensitive to the tnr of the observations.

The previously described selection procedure provides, at least theoretically, a way to analyze large datasets to describe the turbulence climatology in the atmosphere or in the ocean, as suggested by Clayson and Kantha (2008). However, the data resolution, as well as the noise level, both combined in the tnr, are key issues when

applying a Thorpe analysis. A major conclusion of this work is that the data tnr determines the minimum sizes of the detectable overturns by a Thorpe analysis. Clearly, the detected turbulent fraction, as well as the size distribution of the selected overturns, depend heavily on this parameter.

Acknowledgments. The authors wish to acknowledge Centre National d'Études Spatiales (CNES) for operating the balloons in Japan and the Research Institute for Sustainable Humanosphere (RISH) for their contribution in the MUTSI campaign. The authors are also grateful to two anonymous reviewers for helpful comments on the manuscript.

APPENDIX A

Probability for a Noise-Induced Permutation

Let us consider a sample $\{X_1, X_2, \dots, X_n\}$ consisting of a random noise superimposed to a linear trend. The i th bin can be expressed as

$$X_i = s_i + B_i = i\tau + B_i, \quad (\text{A1})$$

where τ is the trend ($\tau = s_{i+1} - s_i$), s_i is the deterministic signal, and B_i is the noise for the i th bin. We assume a normally distributed noise ($B_i \sim N(0, \sigma_N)$) and $\tau \geq 0$. The random variables X_i are independent $X_i \sim N(i\tau, \sigma_N)$, with cumulative distribution function (cdf) F_i .

An inversion between consecutive bins (i.e., permutation) occurs if $X_{i+1} < X_i$. Let p_1 be the probability of such an inversion, that is, $p_1 = \Pr[X_{i+1} < X_i]$. Starting from the conditional probability $\Pr[X_{i+1} < x | X_i = x]$, p_1 reads

$$p_1 = \int_x \Pr[X_{i+1} < x | X_i = x] d \Pr[X_i = x]. \quad (\text{A2})$$

As $X_i = i\tau + B_i$, $d \Pr[X_i = x] = d \Pr[B_i = b] = f(b) db$, f is the probability density function (pdf) of noise (Fig. A1). It then follows that

$$p_1 = \int_b \Pr[B_{i+1} + \tau < b | B_i = b] d \Pr[B_i = b]. \quad (\text{A3})$$

The B_i are independent. Consequently,

$$\Pr[B_{i+1} + \tau < b | B_i = b] = \Pr[B_{i+1} < (b - \tau)] = F(b - \tau), \quad (\text{A4})$$

where F is the cdf of the noise. Finally, we get

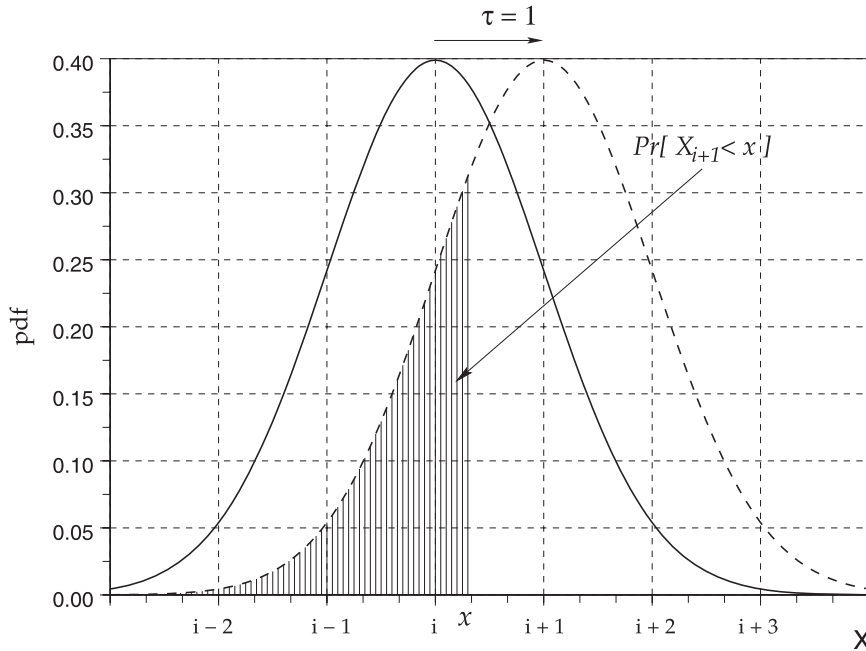


FIG. A1. Probability distributions for two consecutive data bins within a linear trend $\tau = 1$. The conditional probability $\Pr[X_{i+1} < x | X_i = x]$ is the area of the shaded domain.

$$p_1 = \int_{-\infty}^{\infty} F(b - \tau)f(b) db. \tag{A5}$$

for two data bins to permute is a decreasing function of tnr , the run lengths due to noise must also decrease with tnr .

Here, $F(b - \tau)$ is the conditional probability for an inversion of bins i and $i + 1$, given $B_i = b$.

One needs to specify a noise distribution to integrate (A5). For a normally distributed noise, the cdf F reads

$$F(b) = \frac{1}{2} \left[1 + \text{erf} \left(\frac{b}{\sqrt{2}\sigma_N} \right) \right]. \tag{A6}$$

The integration (A5) gives

$$p_1 = \frac{1}{2} \left(1 - \text{erf} \left(\frac{\tau}{2\sigma_N} \right) \right) = \frac{1}{2} \left(1 - \text{erf} \left(\frac{\zeta}{2} \right) \right), \tag{A7}$$

where $\zeta = \tau/\sigma_N$ is the trend-to-noise ratio (tnr) (Fig. A2). The probability p_1 thus depends on the tnr ζ only. The probability for a permutation between two bins, with distant k steps apart reads

$$p_k = \frac{1}{2} \left(1 - \text{erf} \left(\frac{k\zeta}{2} \right) \right). \tag{A8}$$

For $\zeta = 0$, $p_k = 1/2$, and $\forall k$, the probability for a permutation with any bin, is $1/2$. If $\zeta \neq 0$, the probability is a simple function of tnr ζ and of the distance between bins expressed in the steps number k . As the probability

APPENDIX B

Order Statistics

In this appendix, we recall the basic results of the statistics of range, as described by David (1981). Sorting the sample $\{X_1, X_2, \dots, X_n\}$ gives $\{X_{1:n}, X_{2:n}, \dots, X_{n:n}\}$, $X_{i:n}$ defined as the i th order statistics ($i = 1, 2, \dots, n$).

a. Independent identically distributed (iid) variables

First, let us consider the case where the n variables are iid (i.e., $\tau = 0$). Let f and F be the pdf and the cdf of the sample, respectively. The cdf of the r th sorted variable $F_{r:n}$ is obtained by noting that $F_{r:n}(x)$ is the probability that at least r of the X_i is less than or equal to x , that is

$$F_{r:n}(x) = \Pr[X_{r:n} \leq x] = \sum_{i=r}^n \binom{n}{i} F^i(x) [1 - F(x)]^{n-i}. \tag{B1}$$

The pdf is deduced by differentiation:

$$f_{r:n}(x) = \frac{n!}{(r-1)!(n-r)!} f(x) F(x)^{r-1} [1 - F(x)]^{n-r}. \tag{B2}$$

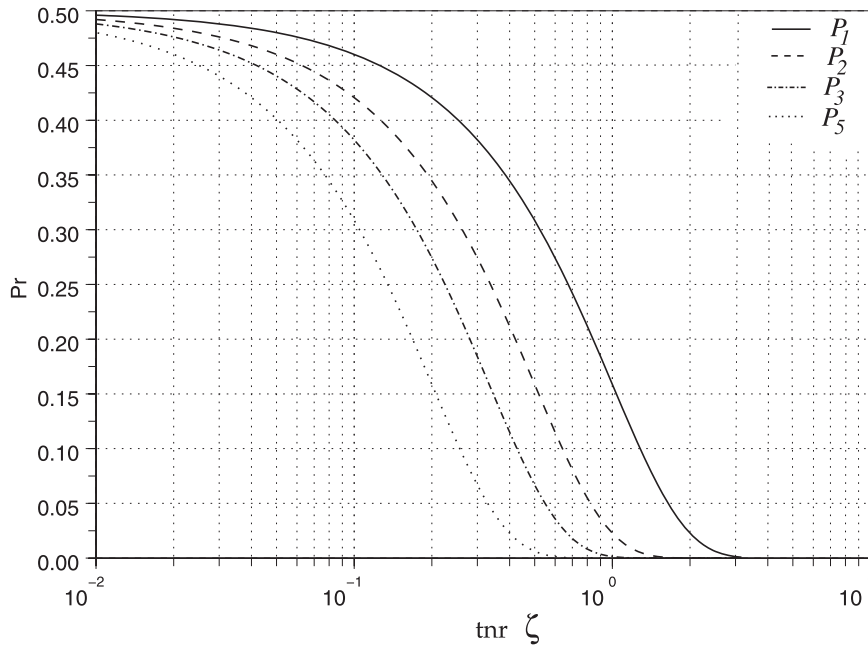


FIG. A2. Probability for a noise-induced permutation between bins as a function of the bins' separation in the initial profile for various tnr ζ . Here, p_1 is the probability for the permutation of two adjacent bins; and p_2, p_3 , and p_5 are for bins separated by 2, 3, and 5 steps, respectively.

The functions f_{rn} and F_{rn} can easily be numerically calculated if one specifies the probability distribution of the sample.

The n range $W(n)$ is defined as the difference between the maximum and minimum of the values in the n sample, that is, $W(n) = X_{n:n} - X_{1:n}$. The cdf of the range of n iid variables is derived by noting that (David 1981)

$$nf(x) dx [F(x+w) - F(x)]^{n-1} \tag{B3}$$

is the probability given x that one of the X_i falls into the interval $(x, x + dx)$ and all of the $n - 1$ remaining X_i fall into $(x, x + w)$. The resulting cdf $F_W(w)$ is obtained by integrating over x :

$$F_W(w) = n \int_{-\infty}^{\infty} f(x) [F(x+w) - F(x)]^{n-1} dx. \tag{B4}$$

The following pdf f_w is deduced:

$$f_W(w) = n(n-1) \int_{-\infty}^{\infty} f(x)f(x+w) \times [F(x+w) - F(x)]^{n-2} dx. \tag{B5}$$

Figure 3 shows the pdf of the n range for a normally distributed parent population for $n = 10, 20$, and 50 . We used this last expression to numerically compute the various percentiles of the range for a normally distributed parent population (Table 2).

b. Non-iid variables

If we now assume that the i th variable has cdf F_i , the cdf of the r th sorted element reads (e.g., David 1981)

$$F_{rn}(x) = \sum_{i=r}^n \sum_{S_i} \prod_{l=1}^i F_{j_l}(x) \prod_{l=i+1}^n (1 - F_{j_l}(x)), \tag{B6}$$

where the summation S_i extends over all permutations j_1, j_2, \dots, j_n of $(1, 2, \dots, n)$, for which $j_1 < j_2 < \dots < j_i$ and

$j_{i+1} < \dots < j_n$. The ensuing complications are considerable. However, this cdf, and the moments, can be numerically evaluated for a limited number of variables (say, $n \leq 20$) without great difficulties if one assumes a linear trend (e.g., Robinson-Cox 1992). The moments of the n range are even functions of the trend τ . For any trend (positive or negative), the n -range expectation is larger than in case of iid variables (i.e., null-trend case).

REFERENCES

Alford, M. H., and R. Pinkel, 2000: Observation of overturning in the thermocline: The context of ocean mixing. *J. Phys. Oceanogr.*, **30**, 805–832.

- Alisse, J.-R., and C. Sidi, 2000: Experimental probability density functions of small-scale fluctuations in the stably stratified atmosphere. *J. Fluid Mech.*, **402**, 137–162.
- Clayson, C. A., and L. Kantha, 2008: On turbulence and mixing in the free atmosphere inferred from high-resolution soundings. *J. Atmos. Oceanic Technol.*, **25**, 833–852.
- Coulman, C., J. Vernin, and A. Fuchs, 1995: Optical seeing—Mechanism of formation of thin turbulent laminae in the atmosphere. *Appl. Opt.*, **34**, 5461–5474.
- Dalaudier, F., C. Sidi, M. Crochet, and J. Vernin, 1994: Direct evidence of sheets in the atmospheric and temperature field. *J. Atmos. Sci.*, **51**, 237–248.
- David, H. A., 1981: *Order Statistics*. John Wiley & Sons, 360 pp.
- Dillon, T. M., 1982: Vertical overturns: A comparison of Thorpe and Ozmidov length scales. *J. Geophys. Res.*, **87**, 9601–9613.
- , 1984: The energetics of overturning structures: Implications for the theory of fossil turbulence. *J. Phys. Oceanogr.*, **14**, 541–549.
- Ferron, B., H. Mercier, K. Speer, A. Gargett, and K. Polzin, 1998: Mixing in the Romanche fracture zone. *J. Phys. Oceanogr.*, **28**, 1929–1945.
- Freeman, H., 1963: Testing statistical hypotheses. *Introduction to Statistical Inference*, Addison-Wesley Publishing Company, 283–305.
- Galbraith, P. S., and D. E. Kelley, 1996: Identifying overturns in CDT profiles. *J. Atmos. Oceanic Technol.*, **13**, 688–702.
- Gargett, A. E., and T. Garner, 2008: Determining Thorpe scales from ship-lowered CTD density profiles. *J. Atmos. Oceanic Technol.*, **25**, 1657–1670.
- Gavrilov, N. M., H. Luce, M. Crochet, F. Dalaudier, and S. Fukao, 2005: Turbulence parameter estimation from high-resolution balloon temperature measurements of the MUTSI-2000 campaign. *Ann. Geophys.*, **23**, 2401–2413.
- Johnson, H. L., and C. Garrett, 2004: Effect of noise on Thorpe scales and run lengths. *J. Phys. Oceanogr.*, **34**, 2359–2372.
- Luce, H., S. Fukao, F. Dalaudier, and M. Crochet, 2002: Strong mixing events observed near the tropopause with the MU radar and high-resolution balloon techniques. *J. Atmos. Sci.*, **59**, 2885–2896.
- Ozmidov, R. V., 1965: On the turbulent exchange in a stably stratified ocean. *Atmos. Ocean Phys.*, **1**, 861–871.
- Piera, J., E. Roget, and J. Catalan, 2002: Turbulent patch identification in microstructure profiles: A method based on wavelet denoising and Thorpe displacement analysis. *J. Atmos. Oceanic Technol.*, **19**, 1390–1402.
- Robinson-Cox, J., 1992: Tables of order statistics of normal random variables under linear trend. *Commun. Stat. Theory Methods*, **21**, 3497–3520.
- St. Laurent, L., and R. W. Schmitt, 1999: The contribution of salt fingers to vertical mixing in the North Atlantic trace release experiment. *J. Phys. Oceanogr.*, **29**, 1404–1424.
- Thorpe, S. A., 1977: Turbulence and mixing in a Scottish loch. *Philos. Trans. Roy. Soc. London*, **286A**, 125–181.
- Timmermans, M.-L., C. Garrett, and E. Carmack, 2003: The thermohaline structure and evolution of the deep waters in the Canada basin, Arctic Ocean. *Deep-Sea Res. I*, **50**, 1305–1321.
- Woods, J. D., 1968: Wave-induced shear instability in the summer thermocline. *J. Fluid Mech.*, **32**, 791–800.